Clean Energy, 2019, 1–12

doi: 10.1093/ce/zky022
Advance Access Publication Date: 6 February 2019
Homepage: https://academic.oup.com/ce

Research Article

Estimating the impact of azimuth-angle variations on photovoltaic annual energy production

Mahmoud Dhimish[1,*] and Santiago Silvestre[2]

[1]Laboratory of Photovoltaics, University of Huddersfield, Queensgate, HD1 3DH, Huddersfield, UK
[2]MNT Group, Electronic Engineering Department, Universitat Politécnica de Catalunya (UPC) BarcelonaTech, C/Jordi Girona 1–3, Campus Nord UPC, 08034 Barcelona, Spain

*Corresponding author. E-mail: mahmoud.dhimish@gmail.com

Abstract

The performance of a photovoltaic (PV) installation is affected by its tilt and azimuth angles, because these parameters change the amount of solar energy absorbed by the surface of the PV modules. Therefore, this paper demonstrates the impact of the azimuth angle on the energy production of PV installations. Two different PV sites were studied, where the first comprises PV systems installed at –13°, –4°, +12° and +21° azimuth angles in different geographical locations, whereas the second PV site included adjacent PV systems installed at –87°, –32°, +2° and +17° azimuth angles. All the investigated PV sites were located in Huddersfield, UK. In summary, the results indicate that PV systems installed between –4° and +2° presented the maximum energy production over the last 4 years, while the worst energy generation were observed for the PV system installed at an azimuth angle of –87°. Finally, the probability projections for all observed azimuth angles datasets have been assessed. Since PV systems are affected by various environmental conditions such as fluctuations in the wind, humidity, solar irradiance and ambient temperature, ultimately, these factors would affect the annual energy generation of the PV installations. For that reason, we have analysed the disparities and the probability of the annual energy production for multiple PV systems installed at different azimuth angles ranging from –90° to +90° degrees, and affected by different environmental conditions. These analyses are based on the cumulative density function modelling technique as well as the normal distribution function.

Keywords: photovoltaics; azimuth angle; energy production; CDF modelling

Introduction

Photovoltaic (PV) system output energy yield strongly depends on weather conditions such as wind speed [1], humidity variations [2], temperature fluctuation and solar irradiance, and some other factors such as dust/dirt [3], hot spots [4, 5], snow [6] and micro cracks [7, 8]. Still, the tilt and azimuth angles of PV installations play a major role in increasing the annual energy production.

Empirical equations were employed in early studies to estimate the optimum tilt angles at different sites, which are only related to local altitude as described by Salim et al. [9]. Later, Mani et al. [10] explained that PV modules should be installed with the tilt angle of 2.8° greater than the latitude.

In 2017, Xu et al. [11] proposed an analysis of the optimum tilt angle for soiled PV panels. It was found that the optimum tilt angle for PV modules was 25.89° to 26.06° in dusty weather conditions. Authors in [12] and [13] estimated the optimum tilt angle for PV panels in Saudi

Received: 30 September, 2018; **Accepted:** 5 December, 2018

Arabia. It was found that the tilt angle of PV panels must be changed during the season of the year to increase the total energy production of PV systems by at least 6.38%.

In other studies, several recommendations for fixed tilt and azimuth angles were suggested based on various locations in the following countries: South Africa [14], Northern Ireland [15], India [16], Iran [17], the USA [18], Turkey [19] and the United Arab Emirates [20].

Various studies on the optimization of tilt angles have considered the effect of cloudiness [21], wind-speed cooling [1], maximizing radiation on flat-plate collectors [22], the clearness index optimization method [23], the radiation-transfer method [24] and maximizing different solar radiations in different geographical locations [25, 26]. These methods are used to draw a relevant map for PV installation tilt and azimuth angles and, thus, enhance the generation of the annual energy of PV systems.

Most recently, in 2018, Antonanzas et al. [27] proposed two predictive models to develop a single-axis tracking system that could determine the optimum position of PV panels. The study has been validated on some European Baseline Surface Radiation Network stations for the year 2015.

But still there is a lack of empirical observations based on various PV systems installed in different locations within a specific regional area. In addition, there are few studies about the impact of the azimuth angle of PV installations based on an annual energy production for several years, which would allow one to draw a relevant conclusion for the ideal angle documentation. Therefore, this article attempts to fill this gap of knowledge found in the literature.

The tilt angle is the angle of the PV modules from the horizontal plane, for a fixed (non-tracking) mounting [28], whereas the azimuth angle is the angle of the PV modules relative to the direction due south; –90° is east, 0° is south and +90° is west [29, 30].

Usually, PV operators/installers use an online application to determine the azimuth angle on the site at its optimum level. However, in residential sites, this cannot be the case since the rooftop is fixed and not flexible. This issue was investigated in 2013 by Kodysh et al. [31]. In this work, a new methodology for estimating solar potential on multiple building rooftops for PV panels is developed. The methodology considers input parameters, such as surface orientation, shadowing effects, elevation and atmospheric conditions, that influenced solar intensity on the Earth's surface. The methodology was implemented for some 212 000 buildings in Knox County, TN, USA.

Later, in 2017, Hong et al. [32] developed a new method for estimating the rooftop PV potential energy based on the tilt and azimuth angle at Gangnam located in Korea. The physical, geographic and technical potentials were estimated for 27 774 buildings. In summary, the total annual physical potential of the rooftop solar PV system in the Gangnam district was determined to be 9 287 982 MWh, whereas the total annual technical potential was found to be 1 130 371 MWh, indicating that only 12.17% of the physical potential can be generated as electricity with the current spatial availability and technology levels. Meanwhile, the average geographic potential in the Gangnam district was found to be 4 964 118 m^2, which accounts for 66.03% of the total rooftop area in the district.

On the other hand, variations in the azimuth angle can lead to significant loss in the output power, and also will affect the PV system by various types of faults. PV faults can be mitigated using various techniques, such as the random forest-based intelligent fault-diagnosis system that is capable of detecting multiple faults in PV arrays, which was developed by Chen et al. [33]. The proposed algorithm ensemble learning algorithm is explored for the detection and diagnosis early faults in PV arrays (including line–line faults, degradation, open circuit and partial shading), which combines multiple learning algorithms to achieve superior diagnostic performance. However, another approach presented in [34] and [35] shows that PV faults can be detected using analysis of the mathematical thresholds such as voltage, current and output power, whereas the fault identification is based on intelligent mathematical modelling techniques.

In addition, the accuracy of the detection of PV faults is enhanced using machine learning techniques, such as artificial neural networks (ANN) [36, 37], fuzzy logic classification systems [38, 39], as well as the wavelet-based classification methods [40].

In this article, first, a database of various PV installations in the region of Huddersfield, shown in Fig. 1, is analysed. From the observed data, it was possible to consider various PV installations with various azimuth angles (ranging from –87° to 21°). Therefore, the impact of various azimuth angles on energy production for PV installations is deliberated.

Since PV systems are affected by various environmental conditions such as wind, humidity, solar irradiance and ambient temperature, these conditions would affect the annual energy generation for the PV installations. For that reason, we have analysed the disparities and the probability of the annual energy production for multiple PV systems installed at different azimuth angles ranging from –90° to +90° degrees.

By contrast with the main motivation of this work, the results could be used in various PV energy sectors, such as PV fault-detection algorithms, PV forecasting and

Fig. 1 Huddersfield town location in the UK.

prediction, PV monitoring and performance analysis, as well as reliability analysis of power systems.

1 Methodology

The azimuth is the PV array's east–west orientation in degrees. In most solar PV energy-calculator tools, an azimuth value of zero is facing the equator in both northern and southern hemispheres; +90° degrees is facing due west and –90° degrees is facing due east. The compass angle shows 180° for south, 90° for east and 270° for west.

In the northern hemisphere, between the latitudes of 23° and 90°, the Sun is always in the south. Therefore, the modules on an array are directed to the south in order to get the most out of the Sun's energy. In the southern hemisphere, it is the opposite.

The meteorological conditions of the location are an important factor to consider. For example, an insolation analysis in Hawaii shows that an array facing to the east could generate more power compared to an array facing south or west [41]. The reason could be the frequent afternoon rains in that location.

For that reason, this paper examines various PV installations with several azimuth angles. However, in order to achieve that, the following conditions were taken into account in order to pick the right PV installations for the study:

- The maximum PV installations are no older than 2 years, since old PV systems tend to have greater degradation rates, thus generating less energy over the years.
- PV module technology is crystalline-silicon (c-Si). This condition was selected to ensure that the operating mechanisms of the PV modules are identical.
- In this research, the examination of the PV installations is based on the difference in the azimuth angle. Therefore, all examined PV installations have the same tilt angle between 40° and 41° degrees.

The examined PV systems are shown in Fig. 2. Two PV sites with various azimuth angles have been considered in this

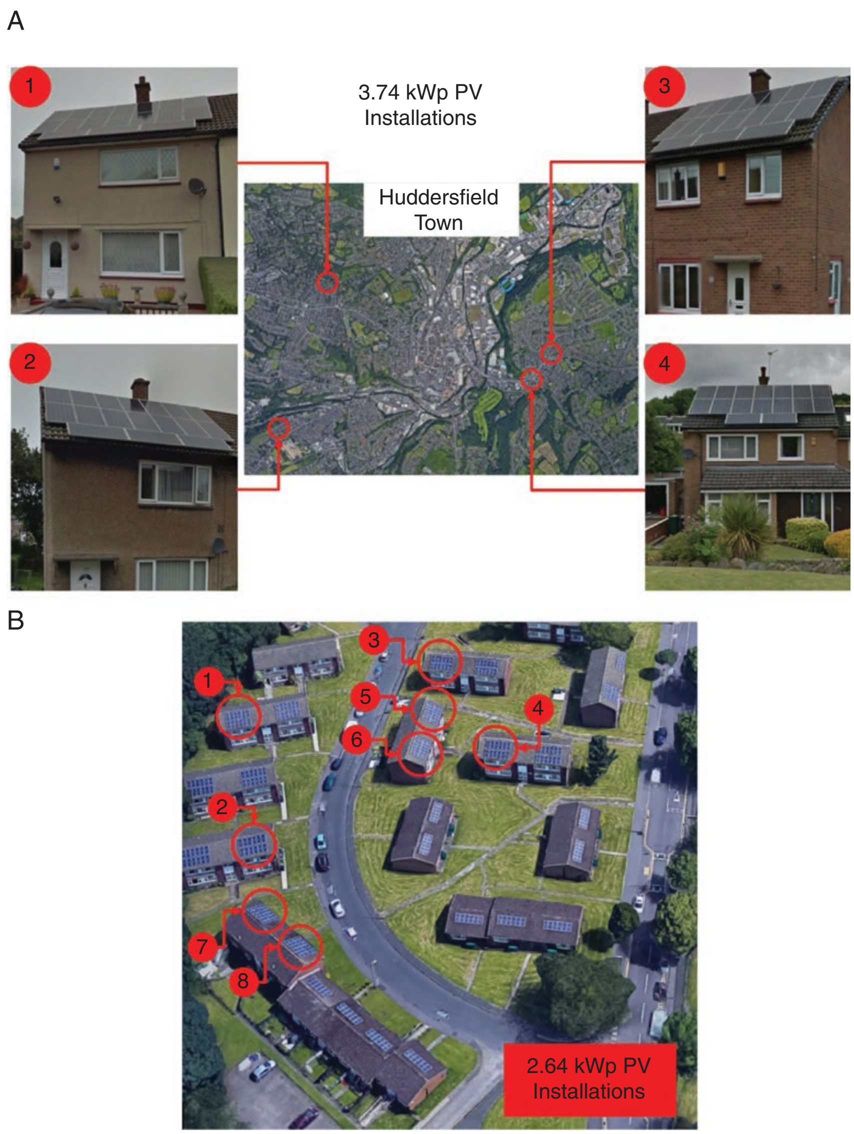

Fig. 2 Examined PV installations. (a) PV site A comprising non-adjacent PV systems, (b) PV site B comprising adjacent PV systems.

study. Fig. 2a shows the first PV installation (referred to as PV site A). PV systems 1, 2, 3 and 4 have –13°, –4°, +12° and +21° azimuth angles, respectively. As shown in Fig. 2a, PV site A is not adjacent. For that reason, we have studied another PV installation (referred to as PV site B) that comprises adjacent PV systems as shown in Fig. 2b.

Fig. 2b shows eight adjacent PV installations that are installed at the same tilt angle of 41°, but with different azimuth angles. The azimuth angles for the PV systems are as follows: +2° for 1 and 2; +17° for 3 and 4; –32° for 5 and 6; –87° for 7 and 8. It is worth noticing that the capacity for all of the studied PV site A is equal to 3.74 kWp, whereas the capacity of PV site B is equal to 2.64 kWp.

Table 1 summarizes the main electrical characteristics of the standard test conditions of the PV modules installed in the studied locations.

Table 1 PV module electrical characteristics

Electrical characteristic	Value
PV peak power	220 W
One PV cell peak power	3.6 W
Voltage at maximum power point (V_{mpp})	28.7 V
Current at maximum power point (I_{mpp})	7.67 A
Open circuit voltage (V_{oc})	36.74 V
Short circuit current (I_{sc})	8.24 A

The data of the examined PV installations were monitored using an OWL Intuition-PV monitoring unit. This monitoring unit transmits the data wirelessly to a local hub installed in the house. The hub logs and saves the data over a shared database with a unique IP address. This unit has the following features:

- transmission frequency: 433 MHz;
- operating range: 30 m;
- transmitter battery life: 2 years;
- sensor suitable to monitor cable rated up to 71 amps.

Additionally, the user is allowed to configure the settings of the PV data. Therefore, the daily, monthly and yearly PV system data can be monitored. Also, it provides graphs showing both historical and peak values, allowing the user to identify when the solar panels have been generating the most energy, and therefore the best times to use power in a day.

2 Results

2.1 PV site A

In order to investigate the difference in the output energy production for multiple PV systems installed at different azimuth angles, firstly, Fig. 3a and b present the monthly irradiance and ambient temperature in the studied location (Huddersfield). It is evident that the irradiance increases in

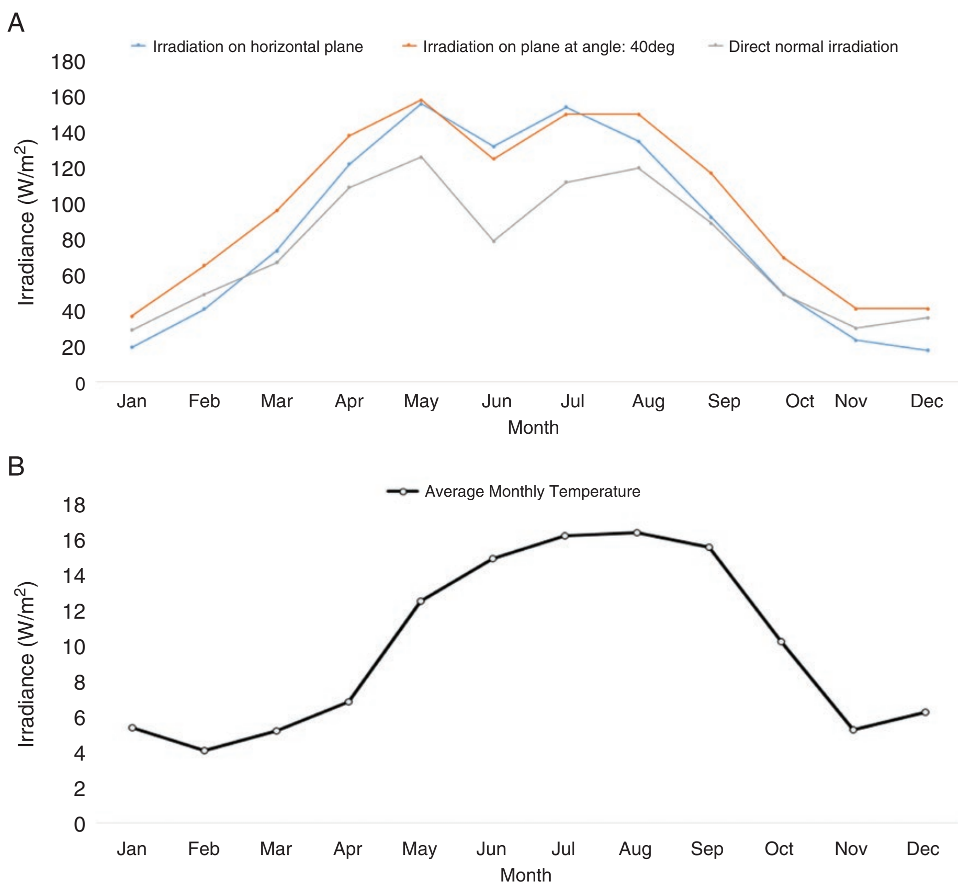

Fig. 3 (a) Monthly irradiance profile in Huddersfield, (b) monthly ambient temperature in Huddersfield.

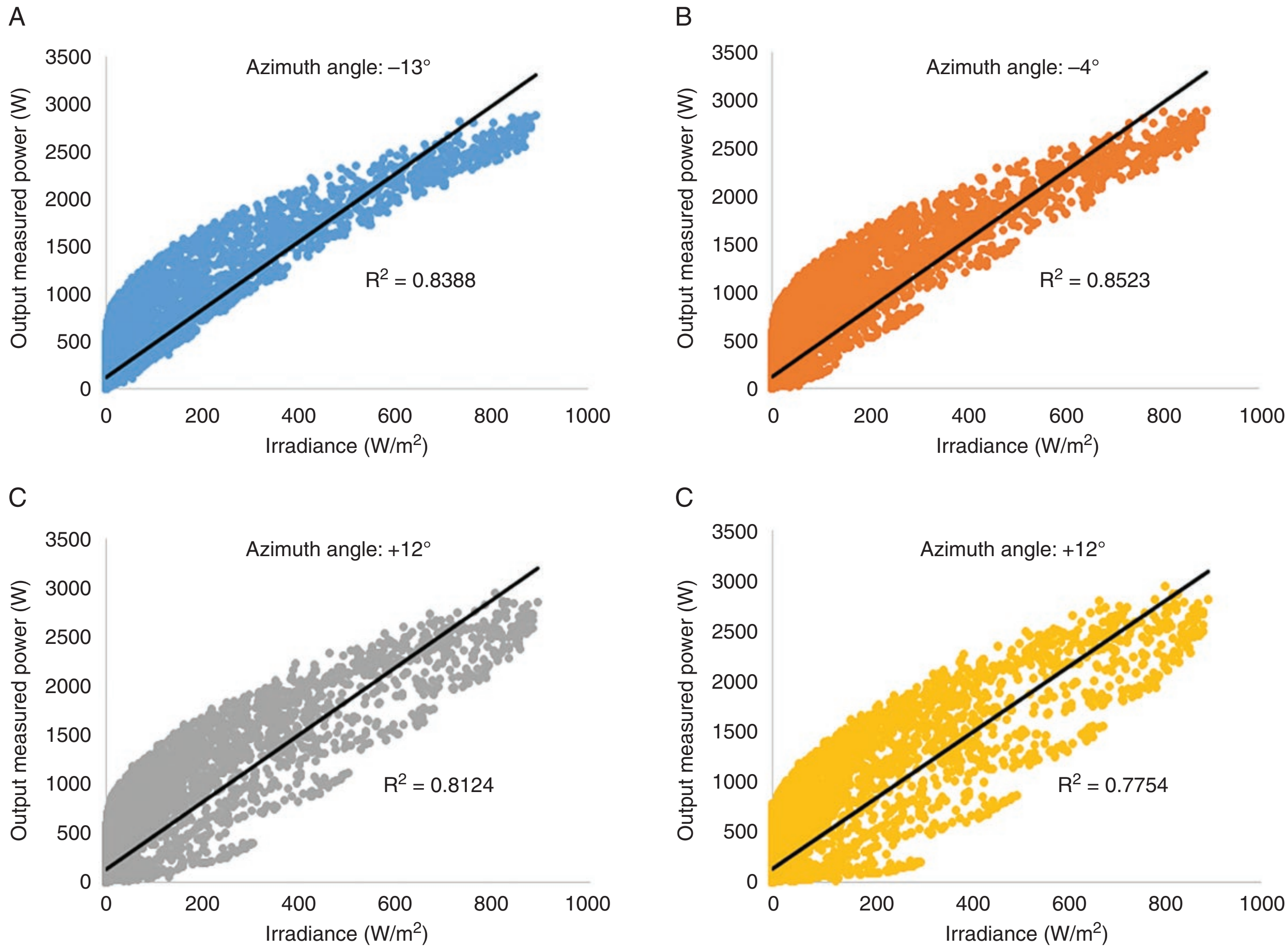

Fig. 4 Irradiance vs. output measured power obtained in PV site A. (a) PV system azimuth angle –13°, (b) PV system azimuth angle –4°, (c) PV system azimuth angle +12°, (d) PV system azimuth angle +21°.

the summer seasons and has low averages in November, December, January and February. In addition, according to Fig. 3b, the average monthly temperature varies between +3.2°C (February) and +16.3°C (September).

A comparison between the PV systems shown previously in Fig. 2a installed at different azimuth angles was carried out. Fig. 3 shows the irradiance vs. output measured power in each of the PV installations analysed. A linear regression fit is presented for each dataset. Therefore, it is possible to compare the PV systems according to the obtained determination factor.

The determination factor, R^2, is a statistical measure of how close the data are to the fitted regression line. A determination factor of 100% indicates that the model explains all the variability of the response data around its mean, where, in fact, this is hard to achieve in PV systems datasets because the measured data relies on the sensor efficiency, solar radiation, temperature variability and many other factors, such as the delay in the data-logging system and the spectrum noise specially added when the PV installations are monitored wirelessly.

The determination factor was measured according to the data samples captured during 2017 for PV site A. It was found that the PV system with azimuth angles of –4° attains the maximum determination factor of 85.23% as shown in Fig. 4b, which means that this PV installation probably generates the maximum output power compared to all other PV systems with different azimuth angles. The minimum value of this parameter was measured for the PV system installed at azimuth angle +21°.

For a better description, in the last 6 years, the annual energy production of PV site A is measured and reported in Fig. 5. It is shown that the PV system installed at azimuth angle –4° shows the maximum energy production over the last 6 years, with an average value of 3537 kWh. The second highest energy production is found for the PV system installed at an azimuth angle of –13° with an average energy production of 3521 kWh. The minimum energy production is observed for the PV system installed at an azimuth angle of +21° with an average value of 3474 kWh, over the last 6 years.

2.2 PV site B

This section describes the performance of PV systems in site B shown previously in Fig. 2b. The PV installations have the following azimuth angles: –87°, –32°, +2° and +17°. The

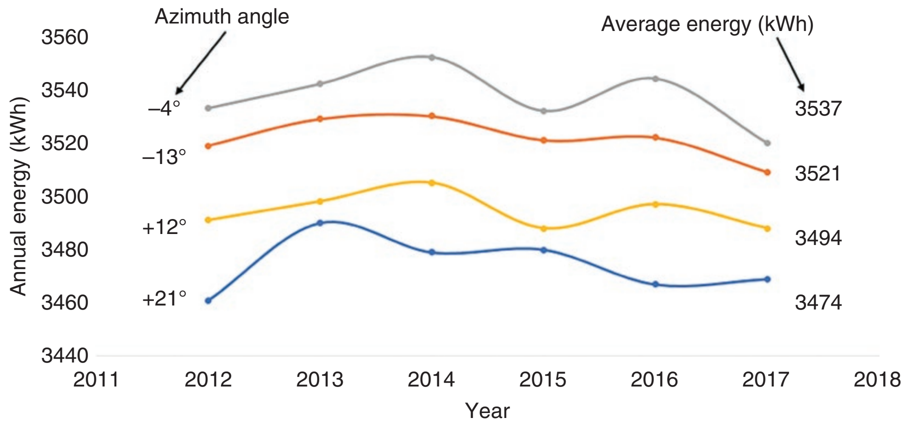

Fig. 5 Annual energy production for PV site A in the last 6 years (2012–17).

data analysed correspond to a period of 4 years between 2014 and 2017. The measured output power of the PV systems with various azimuth angles in the year 2017 as a function of the irradiance for each observed PV system is presented in Fig. 6a–d, whereas the overlap between all measured data is shown in Fig. 6e. As can be seen in the figures, the PV system at an azimuth angle of +2° shows the maximum determination factor of 86.11%. The minimum determination factor is observed for the PV system at an azimuth angle of –87°. This occurred because, at medium and high irradiance (>500 W/m^2) levels, the PV system generates less output power compared to the PV systems installed at azimuth angles of either +2°, +17° or –32°.

The measured data of the irradiance and output power in the interval 2014–16 are shown in Fig. 7. Obtained results indicate that, over the entire time interval considered, the determination factors of the PV systems from maximum to minimum are illustrated as follows:

- azimuth angle +2°: average R^2 = 85.2%, maximum;
- azimuth angle +17°: average R^2 = 83.4%;
- azimuth angle –32°: average R^2 = 77.3%;
- azimuth angle –87°: average R^2 = 48.8%, minimum.

Before moving to the analysis of the annual energy production for each PV installation, the determination factor values suggest that PV installations at an azimuth angle of +2° will generate more energy than other PV installations, since the power production is almost linear with the irradiance profile among the last 4 years of the empirical dataset.

The average monthly energy production by PV systems in site B is shown in Fig. 8a. As can be seen, the PV systems with azimuth angles of +2°, +17° and –32° generate relatively equivalent energy. However, there is a large loss in the monthly energy produced by the PV systems installed at azimuth angle –87° relative to those with other azimuth angles.

The annual energy production in all considered PV systems for site B is given by Fig. 8b. The maximum annual energy based on data observed over the last 4 years (2014–17) is detected for PV systems with azimuth angles of +2°, in the range of 2471–2465 kWh. The second ideal azimuth angle was found to be of +17°, where the PV system generates 2443–2436 kWh yearly.

The minimum energy production is detected in the PV systems installed at azimuth angle –87°. The average annual energy for the considered period of the study is between 2021 and 2019 kWh.

The distribution of the average annual energy production in all PV systems studied for site B is shown in Fig. 9. The maximum and minimum values observed are 2471 and 2019 kWh, respectively. The optimum azimuth angle for the PV installations is observed to be between azimuth angles of +2° and –4°, whereas the minimum value of energy produced was observed for PV systems with azimuth angles of –87°.

A description of the azimuth-angle variations between the south, east and west is shown in Fig. 9b. The probability of the energy production for the PV installations between the south-east and south-west will be described in the next section using the normal distribution function.

3 Probabilistic modelling

In previous sections, the analysis of various azimuth angles was discussed and it was found that the azimuth angle plays a major role in either decreasing or increasing the annual energy generation of a PV system. However, probabilistic modelling incorporating the histogram of all measured energy at various azimuth angles will be evaluated using both normal density function and the cumulative density function (CDF). As shown previously in Fig. 9b and as found in Sections 2 and 3, PV installations facing the south generate the peak annual energy. For that reason, the azimuth-angle variations will be divided for two regions as follows: south-to-east: 0° to –90° and south-to-west: 0° to +90°.

A histogram and a normal distribution function for south-to-east azimuth angles are illustrated in Fig. 10a. As can be seen, the maximum mean energy is observed at 3383 kWh for 0°, whereas the minimum is detected at 2831 kWh for –90°. It is also noticeable that, between the angles 0° and –20°, the annual energy yields are almost identical, at between 3383 and 3353 kWh.

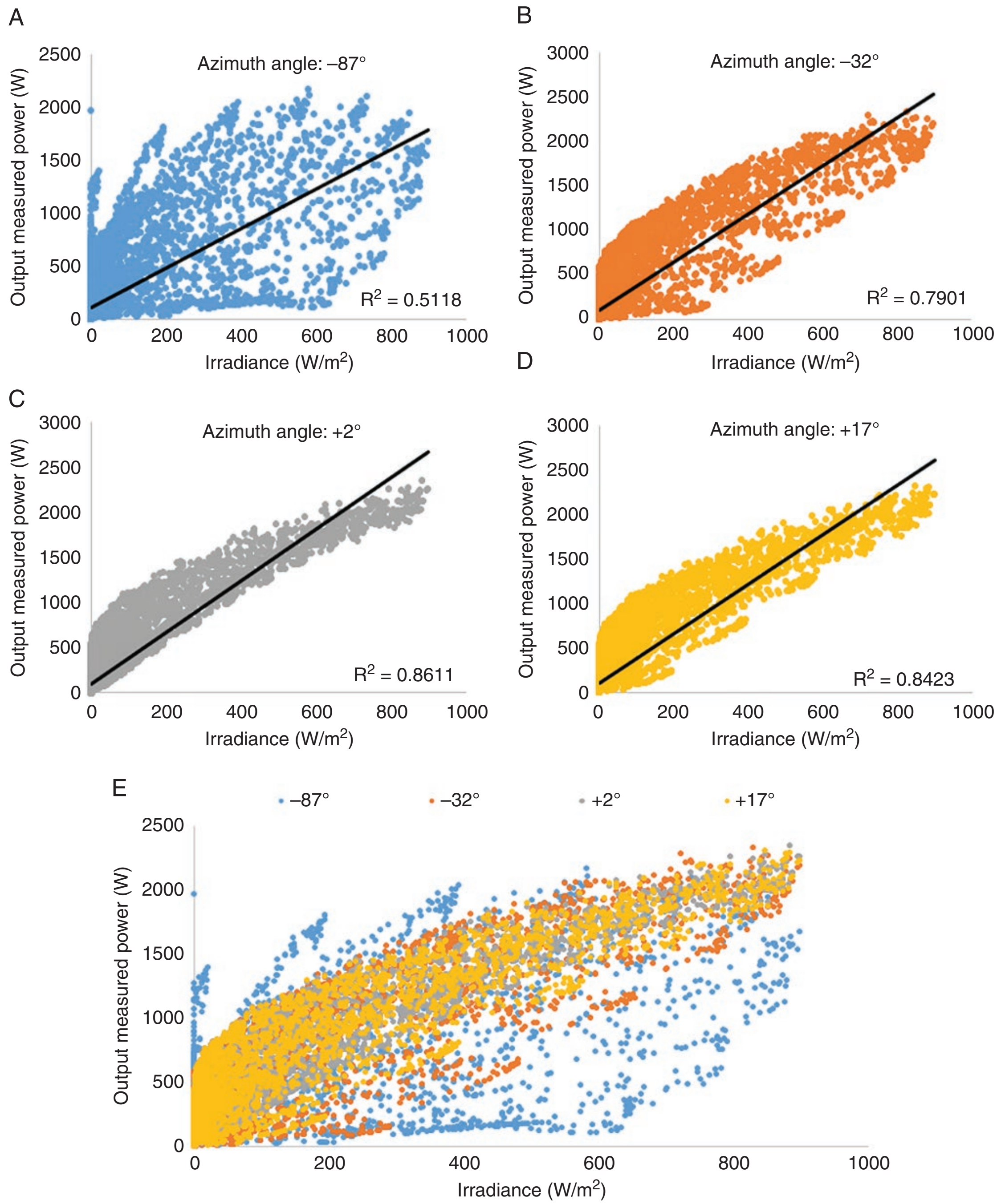

Fig. 6 Irradiance vs. output measured power obtained in PV site B. (a) PV system azimuth angle –87°, (b) PV system azimuth angle –32°, (c) PV system azimuth angle +2°, (d) PV system azimuth angle +17°, (e) overlapping between all PV site B data.

Remarkably, the histogram and the normal distribution of the annual energy for a south-to-west azimuth angle are similar to south-to-east. This result is shown in Fig. 10b. It is evident that there is a high correlation between the annual energy for PV systems installed at 0° to +20°, where the annual energy is always greater than 3300 kWh.

In order to compare between both azimuth-angle categories (south-to-east and south-to-west), all observed samples were combined and plotted as shown in Fig. 10c. This figure shows that the average annual energy for all azimuth angles between 0° to –90° is equal to 3148 kWh. There is slightly less output energy for all azimuth angles between 0° to +90°, which is equal to 3047 kWh.

It is worth noticing that this result does not change the fact that the annual energy yields between +20° and –20° are almost identical for all observed PV installations. However, which angle performs at the optimum probabilistic projection? The answer to this question will be evaluated using the CDF model for all data samples between azimuth angles of +20° and –20°. Therefore, it is possible to talk about how 'likely' or 'unlikely' a PV system at a specific azimuth angle would generate energy at a specific threshold.

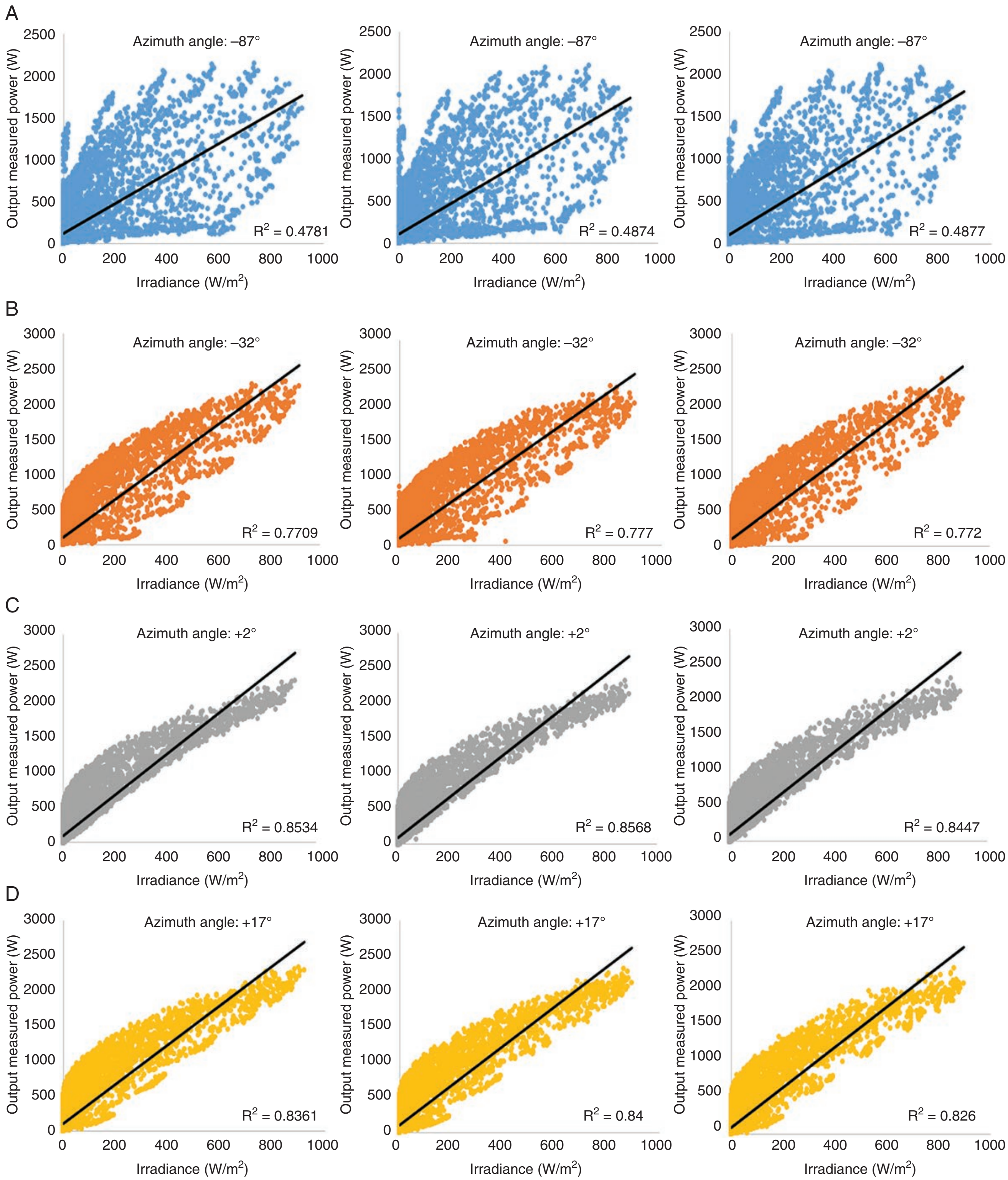

Fig. 7 Irradiance vs. measured power obtained in PV site B (2014, 2015 and 2016 left to right). (a) PV system azimuth angle –87°, (b) PV system azimuth angle –32°, (c) PV system azimuth angle +2°, (d) PV system azimuth angle +17°.

The output CDF plots are shown in Table 2. The CDF plots demonstrate the probability of a PV system installed at specific azimuth angle to maintain a specific annual energy. According to Table 2, the CDF plots are shown at two specific projections of 90 and 70%. Statistically sparking, 70% is a reasonable probability selection, since it has been used as a rule of thumb in order to incorporate the data of a CDF model to actual representation of its findings, which is a practice that has been widely utilized [42–44].

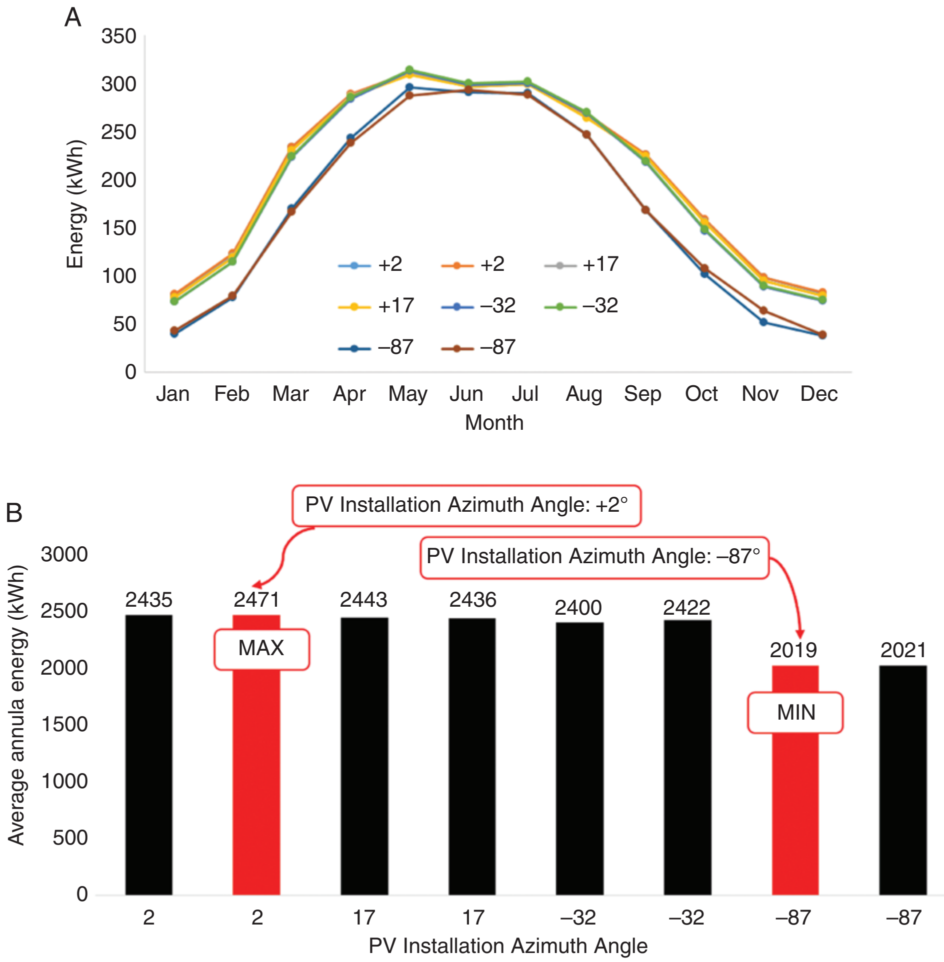

Fig. 8 (a) Average monthly energy production between 2014 and 2017 by PV systems in site B, (b) average annual energy production between 2014 and 2017 generated by PV systems in PV site B.

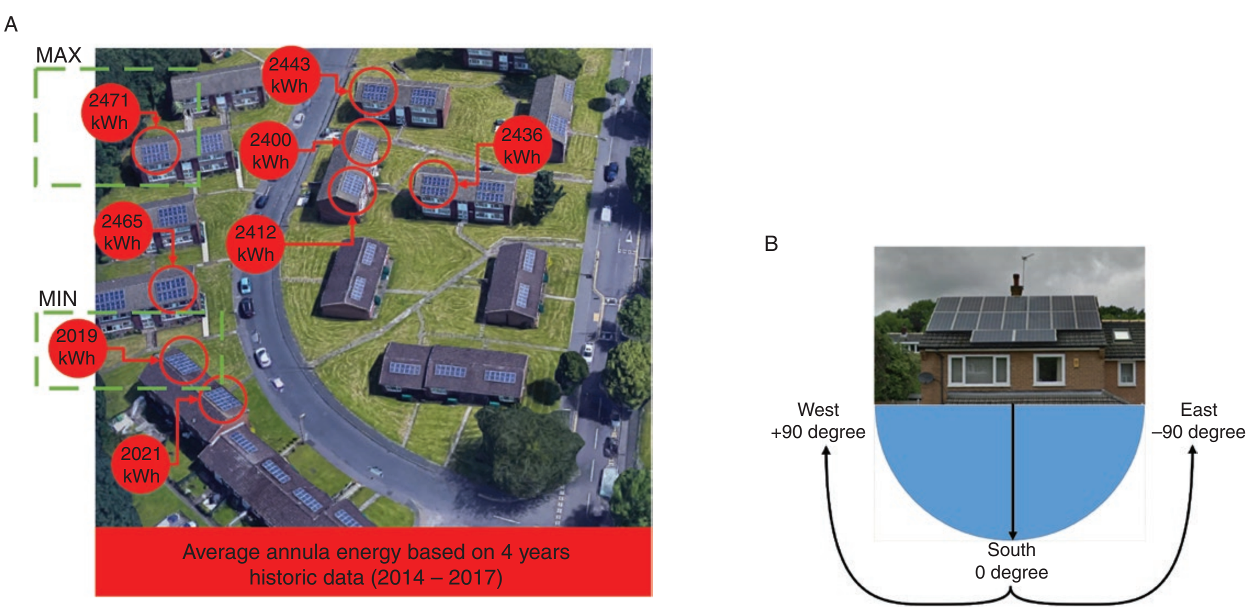

Fig. 9 (a) Average annual energy production for PV systems in site B, (b) azimuth-angle variations (south, east and west).

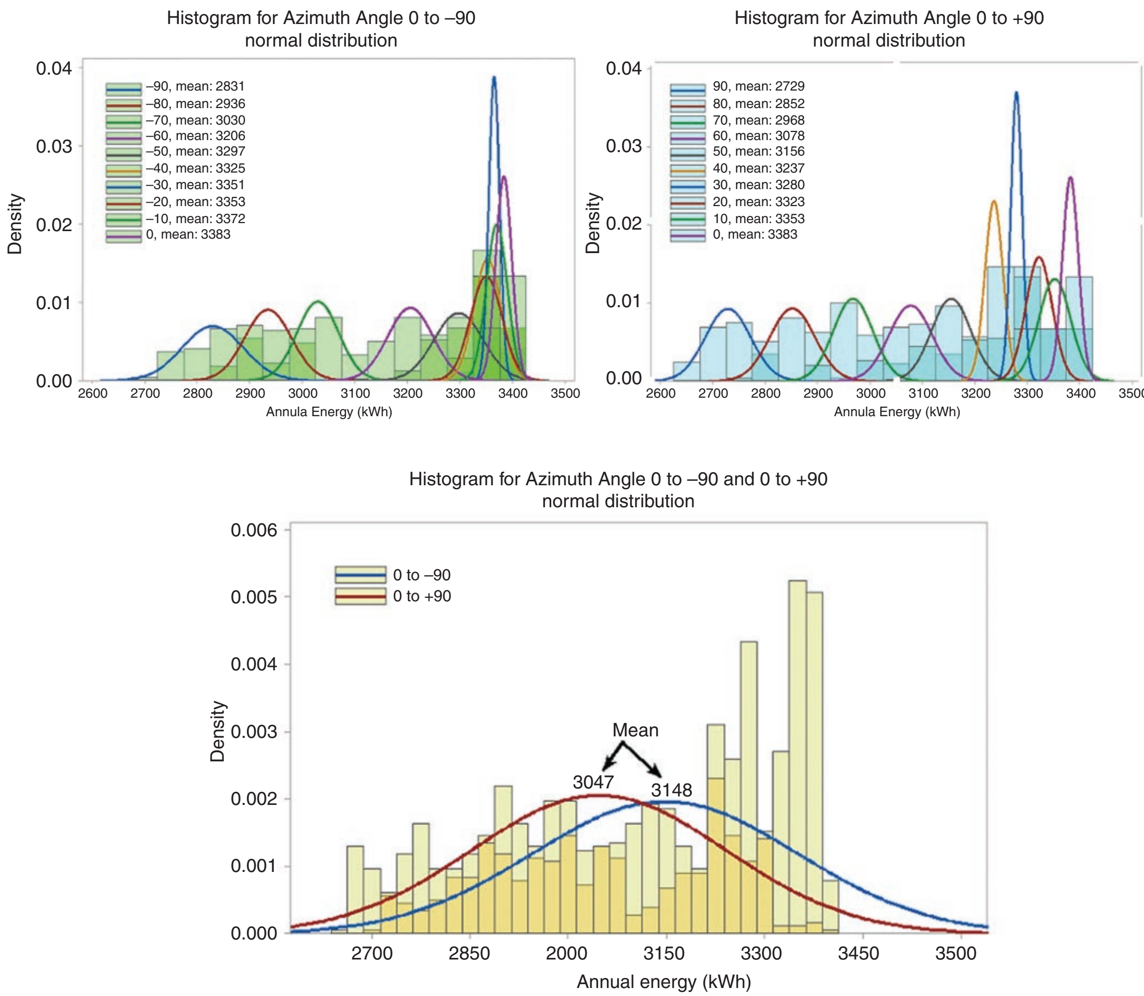

Fig. 10 Histogram and normal distribution density function for the PV annual energy, all PV installation capacities are equal to 3.6 kWp installed at tilt angle 41°. (a) Azimuth angle from 0° to –90°, (b) azimuth angle from 0° to +90°, (c) comparison between the normal distribution density functions for PV azimuth angle from 0° to –90° and 0° to +90°.

According to the CDF models, there is 90 and 70% chance that PV systems installed at 0° would generate an annual energy of 3403 and 3391 kWh, respectively. This annual energy projection is the highest among all other tested azimuth angles. The minimum projections are observed at an azimuth angle of +20° at 3356 (90%) and 3337 (70%) kWh.

Table 2 illustrates that, at 90 and 70% projection rates, the optimum azimuth angle remained at 0°. On the other hand, Table 3 shows the CDF plot projections at 20%. In this scenario, there is a 20% chance that the PV systems installed at an azimuth angle of 0° would generate 3371 kWh annually. Various results obtained for the observed azimuth angles are as follows:

- –10°: 3353 kWh;
- +10°: 3328 kWh;
- –20°: 3325 kWh;
- +20°: 3302 kWh.

Remarkably, the second optimum azimuth angle is observed at –10°. There is 90 and 70% chance that a PV system installed at these azimuth angles would generate an annual energy of 3396 and 3381 kWh, respectively.

4 Conclusion

This paper analysed the impact of the azimuth angle on the energy production of PV installations. Two different PV sites, namely site A and site B, were studied. Site A comprised PV systems installed at –13°, –4°, +12° and +21° azimuth angles in different geographical locations, whereas PV site B included adjacent PV systems installed at –87°, –32°, +2° and +17° azimuth angles.

In PV site A, the PV system installed at an azimuth angle of –40° generated the maximum energy production over the considered period (2012–17), where its average energy was equal to 3537 kWh. The second highest energy production was found for the PV system installed at an azimuth angle of –13°, with an average energy production of 3521 kWh. The minimum energy production was observed for the PV system installed at an azimuth angle of +21°, with an average energy production of 3474 kWh over the studied period.

Table 2 CDF model output results at 90 and 70% projection rates

CDF 90%					
Azimuth angle	+20°	+10°	0°	−10°	−20°
Output energy (kWh)	3356	3393	3403	3396	3388
CDF output results	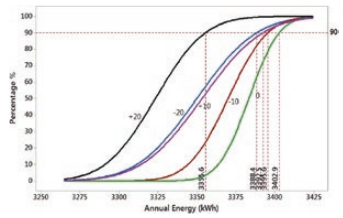				
CDF 70%					
Azimuth angle	+20°	+10°	0°	−10°	−20°
Output energy (kWh)	3337	3369	3391	3381	3367
CDF output results	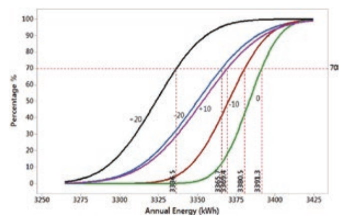				

Table 3 CDF model output results at 20% projection rate

CDF 20%					
Azimuth angle	+20°	+10°	0°	−10°	−20°
Output energy (kWh)	3302	3328	3371	3353	3325
CDF output results	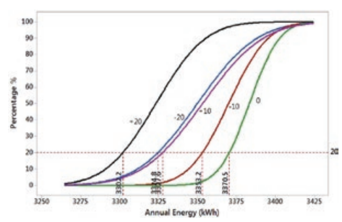				

Results obtained for PV site B over the same period of 4 years showed a maximum annual energy production for PV systems installed at azimuth angles of +2° where the annual energy produced was in the range of 2471–2465 kWh. The second ideal azimuth angle was found to be at +17°, where the PV system generated yearly energy production in the range of 2443–2436 kWh. The minimum energy production was observed in PV systems installed at an azimuth angle of –87°, with an average annual energy production in the range of 2021–2019 kWh.

Conflict of interest statement. None declared.

References

[1] Cludius J, Hermann H, Matthes FC, et al. The merit order effect of wind and photovoltaic electricity generation in Germany 2008–2016: estimation and distributional implications. *Energy Econ* 2014; 44:302–13.

[2] Kazem HA, Chaichan MT. Effect of humidity on photovoltaic performance based on experimental study. *International Journal of Applied Engineering Research (IJAER)* 2015; 10:43572–7.

[3] Silvestre S, Tahri A, Tahri F, et al. Evaluation of the performance and degradation of crystalline silicon-based photovoltaic modules in the Saharan environment. *Energy* 2018; 152:57–63.

[4] Dhimish M, Holmes V, Mehrdadi B, et al. PV output power enhancement using two mitigation techniques for hot spots and partially shaded solar cells. *Electr Power Syst Res* 2018; 158:15–25.

[5] Dhimish M, Holmes V, Mather P, et al. Novel hot spot mitigation technique to enhance photovoltaic solar panels output power performance. *Sol Energy Mater Sol Cells* 2018; 179:72–9.

[6] Chen M, Wu S, Wang H, et al. Study of ice and snow melting process on conductive asphalt solar collector. *Sol Energy Mater Sol Cells* 2011; 95:3241–50.

[7] Dhimish M, Holmes V, Mather P, et al. Development of 3D graph-based model to examine photovoltaic micro cracks. *J Sci Adv Mater Devices* 2018; 3:380–8.

[8] Dhimish M, Holmes V, Dales M, et al. Effect of micro cracks on photovoltaic output power: case study based on real time long term data measurements. *IET Micro & Nano Letters* 2017; 12:803–7.

[9] Salim AA, Huraib FS, Eugenio NN. PV power-study of system options and optimization. *InEC Photovoltaic Solar Conference* 1988; 8:688–92.

[10] Mani M, Pillai R. Impact of dust on solar photovoltaic (PV) performance: research status, challenges and recommendations. *Renew Sustain Energy Rev* 2010; 14:3124–31.

[11] Xu R, Ni K, Hu Y, et al. Analysis of the optimum tilt angle for a soiled PV panel. *Energy Convers Manage* 2017; 148:100–9.

[12] Kaddoura TO, Ramli MA, Al-Turki YA. On the estimation of the optimum tilt angle of PV panel in Saudi Arabia. *Renew Sustain Energy Rev* 2016; 65:626–34.

[13] Sedraoui K, Ramli MA, Mehedi IM, et al. Optimum orientation and tilt angle for estimating performance of photovoltaic modules in western region of Saudi Arabia. *J Renewable Sustainable Energy* 2017; 9:023702.

[14] Le Roux WG. Optimum tilt and azimuth angles for fixed solar collectors in South Africa using measured data. *Renew Energy* 2016; 96:603–12.

[15] Mondol JD, Yohanis YG, Norton B. The impact of array inclination and orientation on the performance of a grid-connected photovoltaic system. *Renew Energy* 2007; 32:118–40.

[16] Yadav P, Chandel SS. Comparative analysis of diffused solar radiation models for optimum tilt angle determination for Indian locations. *Appl Sol Energy* 2014; 50:53–9.

[17] Jafarkazemi F, Ali Saadabadi S, Pasdarshahri H. The optimum tilt angle for flat-plate solar collectors in Iran. *J Renewable Sustainable Energy* 2012; 4:013118.

[18] Lave M, Kleissl J. Optimum fixed orientations and benefits of tracking for capturing solar radiation in the continental United States. *Renew Energy* 2011; 36:1145–52.

[19] Bakirci K. General models for optimum tilt angles of solar panels: Turkey case study. *Renew Sustain Energy Rev* 2012; 16:6149–59.

[20] Jafarkazemi F, Saadabadi SA. Optimum tilt angle and orientation of solar surfaces in Abu Dhabi, UAE. *Renew Energy* 2013; 56:44–9.

[21] Armstrong S, Hurley WG. A new methodology to optimise solar energy extraction under cloudy conditions. *Renew Energy* 2010; 35:780–7.

[22] Stanciu C, Stanciu D. Optimum tilt angle for flat plate collectors all over the world: a declination dependence formula and comparisons of three solar radiation models. *Energy Convers Manage* 2014; 81:133–43.

[23] Rawat R, Kaushik SC, Lamba R. A review on modeling, design methodology and size optimization of photovoltaic based water pumping, standalone and grid connected system. *Renew Sustain Energy Rev* 2016; 57:1506–19.

[24] Smith CJ, Forster PM, Crook R. An all-sky radiative transfer method to predict optimal tilt and azimuth angle of a solar collector. *Sol Energy* 2016; 123:88–101.

[25] Dhimish M, Holmes V, Mather P, et al. Preliminary assessment of the solar resource in the United Kingdom. *Clean Energy* 2018; 2:112–25.

[26] Stanciu D, Stanciu C, Paraschiv I. Mathematical links between optimum solar collector tilts in isotropic sky for intercepting maximum solar irradiance. *J Atmos Sol-Terr Phys* 2016; 137:58–65.

[27] Antonanzas J, Urraca R, Martinez-de-Pison FJ, et al. Optimal solar tracking strategy to increase irradiance in the plane of array under cloudy conditions: a study across Europe. *Sol Energy* 2018; 163:122–30.

[28] Alsadi SY, Nassar YF. Estimation of solar irradiance on solar fields: an analytical approach and experimental results. *IEEE Trans Sustainable Energy* 2017; 8:1601–8.

[29] Sidek MH, Azis N, Hasan WZ, et al. Automated positioning dual-axis solar tracking system with precision elevation and azimuth angle control. *Energy* 2017; 124:160–70.

[30] Mahmoud Y, El-Saadany EF. A Novel MPPT Technique based on an image of PV modules. *IEEE Trans Energy Convers* 2017; 32:213–21.

[31] Kodysh JB, Omitaomu OA, Bhaduri BL, et al. Methodology for estimating solar potential on multiple building rooftops for photovoltaic systems. *Sustain Cities Soc* 2013; 8:31–41.

[32] Hong T, Lee M, Koo C, et al. Development of a method for estimating the rooftop solar photovoltaic (PV) potential by analyzing the available rooftop area using Hillshade analysis. *Appl Energy* 2017; 194:320–32.

[33] Chen Z, Han F, Wu L, et al. Random forest based intelligent fault diagnosis for PV arrays using array voltage and string currents. *Energy Convers Manage* 2018; 178:250–64.

[34] Dhimish M, Holmes V, Mehrdadi B, et al. Multi-layer photovoltaic fault detection algorithm. *High Voltage* 2017; 2:244–52.

[35] Wu L, Chen Z, Long C, et al. Parameter extraction of photovoltaic models from measured IV characteristics curves using a hybrid trust-region reflective algorithm. *Appl Energy* 2018; 232:36–53.

[36] Beniwal R, Gupta HO, Tiwari GN. A generalized ANN model for reliability analysis of a semitransparent photovoltaic solar module with cost modeling. *J Comput Electron* 2018; 17:1167–75.

[37] Dhimish M, Holmes V, Mehrdadi B, et al. Comparing Mamdani Sugeno fuzzy logic and RBF ANN network for PV fault detection. *Renew Energy* 2018; 117:257–74.

[38] Belaout A, Krim F, Mellit A, et al. Multiclass adaptive neuro-fuzzy classifier and feature selection techniques for photovoltaic array fault detection and classification. *Renew Energy* 2018; 127:548–58.

[39] Dhimish M, Holmes V, Mehrdadi B, et al. Photovoltaic fault detection algorithm based on theoretical curves modelling and fuzzy classification system. *Energy* 2017; 140:276–90.

[40] Yi Z, Etemadi AH. Fault detection for photovoltaic systems based on multi-resolution signal decomposition and fuzzy inference systems. *IEEE Trans Smart Grid* 2017; 8:1274–83.

[41] Habte A, Sengupta M, Lopez A. *Evaluation of the National Solar Radiation Database (NSRDB): 1998–2015*. Golden, CO: National Renewable Energy Lab (NREL), 2017.

[42] Nikmehr N, Najafi-Ravadanegh S. Optimal operation of distributed generations in micro-grids under uncertainties in load and renewable power generation using heuristic algorithm. *IET Renew Power Gener* 2015; 9:982–90.

[43] Dhimish M, Mather P, Holmes V. Evaluating power loss and performance ratio of hot-spotted photovoltaic modules. *IEEE Trans Electron Devices* 2018; 65:5419–27.

[44] Taylor J, Leloux J, Hall LM, et al. Performance of distributed PV in the UK: a statistical analysis of over 7000 systems. *31st European Photovoltaic Solar Energy Conference and Exhibition* 2016:2263–68.